Multi-site infective endocarditis complicated by a left ventricular abscess and pseudoaneurysm: A case report

Mahima Tyagi,[1] Tori Seasor,[2] Mark S Slaughter[3] and Dinesh K Kalra[1]

1. Division of Cardiology, Department of Medicine, University of Louisville, Louisville, KY, USA; 2. Department of Pathology and Laboratory Medicine, University of Louisville, Louisville, KY, USA; 3. Department of Cardiovascular and Thoracic Surgery, University of Louisville, Louisville, KY, USA

https://doi.org/https://doi.org/10.17925/HI.2026.20.2.1

Background: Native valve infective endocarditis (IE) is a relatively rare condition with an incidence of 3–7 cases per 100,000 person-years. Even rarer is the occurrence of left ventricular pseudoaneurysm (LVP) as a complication of IE. **Case summary:** A 52-year-old man with insulin-dependent diabetes and well-controlled human immunodeficiency virus was diagnosed with IE with mitral valve vegetations and a left ventricular myocardial abscess, causing an LVP. This diagnosis was confirmed using cardiovascular magnetic resonance imaging (CMR), cardiovascular computed tomography angiography (CCTA) and transesophageal echocardiogram. He was treated with antibiotics, surgical LVP repair and bioprosthetic mitral valve replacement. **Discussion:** LVP is a rare and potentially lethal condition, typically occurring in the setting of myocardial infarction and only rarely secondary to IE. This case demonstrates the critical role of multimodality imaging, including echocardiography, CMR and CCTA, which was instrumental for accurate diagnosis, surgical planning and successful repair.

Keywords

Cardiac magnetic resonance imaging (MRI), cardiac computed tomography (CT) angiography, endocarditis, left ventricular pseudoaneurysm, myocardial abscess, streptococcal bacteremia

Disclosures: Mahima Tyagi, Tori Seasor, Mark S Slaughter and Dinesh K Kalra have no financial or non-financial relationships or activities to declare in relation to this article.

Acknowledgements: No artificial intelligence (AI) or large language model (LLM) tools were used in the development of this article.

Review process: Double-blind peer review.

Compliance with ethics: Written informed consent was obtained from the patient for publication of this case report and accompanying images. Institutional Review Board approval was not required for this single-patient case report in accordance with institutional policy. The research was conducted in accordance with the principles outlined in the Helsinki Declaration of 1964 and its later amendments.

Data availability: All relevant clinical data supporting the findings of this case report, including laboratory values and imaging findings, are included within the article. Additional patient data are not publicly available in order to protect patient confidentiality.

Authorship: All named authors meet the criteria of the International Committee of Medical Journal Editors for authorship for this manuscript, take responsibility for the integrity of the work as a whole and have given final approval for the version to be published.

Access: This article is freely accessible at touchCARDIO.com. © Touch Medical Media 2026.

Received: 12 March 2026

Accepted: 17 April 2026

Published online: 19 July 2026

Citation: *Heart International.* 2026;20(2):49–53

Corresponding author: Dinesh K Kalra, Division of Cardiology, Department of Medicine, University of Louisville, School of Medicine, Rudd Heart & Lung Center, 201 Abraham Flexner Way, Suite 600, Louisville, KY 40202, USA. E: dinesh.kalra@louisville.edu

Support: No funding was received for the publication of this article.

Native valve infective endocarditis (IE) is rare, with an incidence of 3–7 cases per 100,000 person-years.[1,2] Cardiac structural complications from local infection extension include valvular destruction, peri-annular abscess and fistula formation. Left ventricular pseudoaneurysm (LVP) from IE is exceedingly rare, occurring in <1% of cases, and is associated with high morbidity and mortality. Diagnosis is challenging due to nonspecific symptoms and potentially nondiagnostic initial transthoracic echocardiography (TTE). Advanced cardiac imaging, including transesophageal echocardiography (TEE), cardiovascular computed tomography angiography (CCTA) and cardiovascular magnetic resonance (CMR), provides complementary structural and tissue characterization, improving diagnostic accuracy and guiding operative planning. We present a case of native mitral valve IE complicated by myocardial abscess and LVP, in which multimodality imaging was essential for diagnosis and successful surgical management.

Case summary

A 52-year-old man with insulin-dependent diabetes mellitus and human immunodeficiency virus (HIV) on antiretroviral therapy presented to the emergency department with 2 weeks of fatigue, myalgias and increased urinary frequency. He confirmed medication adherence and denied intravenous drug use, recent travel or pet exposure. His medical history was notable for well-controlled HIV (diagnosed in 2015, acquired through male-to-male sexual contact) managed with bictegravir, emtricitabine and tenofovir alafenamide plus insulin-dependent type 2 diabetes, hypertension and hyperlipidemia. He had no prior cardiac surgery, dental caries, valvular or rheumatic disease or chest radiation.

He was febrile (101.9°F), tachycardic (108 beats/min) and tachypneic (22 breaths/min) with blood pressure 120/82 mmHg and oxygen saturation 94% on room air. Examination revealed tachycardia and an S4 gallop, but no murmurs, oropharyngeal lesions, rashes or organomegaly. Laboratory evaluation (*Table 1*) showed an elevated high-sensitivity troponin I level, leukocytosis and hyperglycemia. Urine studies revealed glucosuria, bacteriuria, red blood cells, white blood cells and a positive leukocyte esterase. His CD4+ count was 311 cells/μL (≤200 cells/μL defines acquired immunodeficiency syndrome), with an undetectable HIV viral load. Electrocardiogram (ECG) showed ST-segment elevation and PR segment depression in leads I, II, aVF and V4–V6.

Differential diagnosis

The differential diagnosis was broad and included infections (viral, bacterial, fungal and opportunistic), malignancy, autoimmune and inflammatory syndromes, type 2 non-ST-elevated myocardial infarction and myopericarditis.

Table 1: Laboratory parameters at presentation (Day 1)

Laboratory test	Value	Reference range
Venous blood gas		
pH	7.403	7.31–7.41
pCO2	41.5 mmHg	41–51 mmHg
pO2	24 mmHg	25–40 mmHg
HCO3	25.9 mmol/L	20–24 mmol/L
Blood		
Sodium	127 mmol/L	136–145 mmol/L
Potassium	5.0 mmol/L	3.5–5.1 mmol/L
Chloride	89 mmol/L	98–110 mmol/L
Carbon dioxide	24 mmol/L	21–31 mmol/L
Anion gap	14	2–12
Glucose	581 mg/dL	74–99 mg/dL
Blood urea nitrogen	23 mg/dL	7–25 mg/dL
Serum creatinine	0.96 mg/dL (patient baseline 0.94 mg/dL)	0.7-1.3 mg/dL
Calcium level	9.4 mg/dL	8.6–10.2 mg/dL
Magnesium level	1.9 mg/dL	1.9–2.7 mg/dL
Phosphorus	3.4 mg/dL	2.5–5.0 mg/dL
Protein total	7.6 g/dL	6.4–8.9 g/dL
Albumin level	3.1 g/dL	3.5–5.2 g/dL
Bilirubin total	0.7 mg/dL	0.3–1.0 mg/dL
Alkaline phosphatase	267 units/L	34–104 units/L
AST	35 units/L	13–39 units/L
ALT	26 units/L	0–32 units/L
Lactic acid	1.4 mmol/L	0.5–1.9 mmol/L
Beta hydroxybutyrate	2.58 mmol/L	0–0.25 mmol/L
CD4+ count	311 cells/µL	≥200 cells/µL
HIV viral load	Undetectable	Nil
hsTnI	206 ng/L	≤19 ng/L
BNP	269 pg/mL	5–100 pg/mL
WBC	14.7×10^3/µL	$4.0–10.8\times10^3$/µL
Hemoglobin	13.3 g/dL	13.5–17.5 g/dL
Hematocrit	41.2%	41–53%
MCV	80.6 fL	80–100 fL
Platelets	464×10^3/µL	$140–420\times10^3$/µL
HbA1c	14%	<6.4%
Urinalysis		
Glucose	>1,000 mg/dL	Negative
RBC	5–9 per hpf	0–2 per hpf
WBC	30–49 per hpf	0–5 per hpf
Bacteria	1+	Negative
Leucocyte esterase	250 leu/µL	Negative
Nitrite	Negative	Negative

ALT = alanine aminotransferase; AST = aspartate aminotransferase; BNP = B-type natriuretic peptide; HbA1c = glycated hemoglobin; HIV = human immunodeficiency virus; hpf = high power field; hsTnI = high-sensitivity troponin I; MCV = mean corpuscular volume; RBC = red blood cells; WBC = white blood cells.

Investigations

A TTE was done, which was of poor quality but showed no gross abnormalities. Two sets of blood cultures grew Gram-positive cocci. The patient was started on intravenous ceftriaxone for presumed urosepsis. Two days later, blood cultures speciated into group B Streptococcus (*Streptococcus agalactiae*) susceptible to ceftriaxone; urine cultures grew the same pathogen. Due to persistent fevers, additional blood cultures were obtained on days 3 and 9 of hospitalization, both of which showed no microbial growth. Given the abnormal ECG and troponin, there was concern for myopericarditis or myocardial injury; thus, CMR was performed on hospital day 5. This demonstrated a 1.7×1.0 cm mass on the posterior leaflet of the mitral valve (MV), an anterior left ventricular wall intramyocardial mass measuring 2.5×1.0 cm concerning for an abscess and mid-inferolateral left ventricular wall thinning with pericardial adhesions suggestive of a focal, sealed wall rupture, i.e. an LVP (*Figure 1A, B*). Additional findings included splenic infarcts and a moderate pericardial effusion causing right ventricular collapse.

To better determine the etiology of the LVP and rule out coronary artery disease, CCTA was obtained on hospital day 7. The CCTA showed a coronary artery calcium score of 1 Agatston unit, a non-obstructive, partially calcified, atherosclerotic plaque in the proximal circumflex artery and confirmed the LVP involving the mid- and apical inferolateral segments with a serpiginous tract in the wall. It also identified a pedunculated vegetation on the posterior MV leaflet and a moderate circumferential pericardial effusion with attenuation consistent with serosanguineous fluid (*Figure 1C, D*). Next, a TEE was performed on hospital day 8 to further characterize the MV mass. This showed a vegetation on the posterior mitral leaflet, measuring 2.0×1.2 cm on the P1–P2 scallops, and on the anterior mitral leaflet, measuring 0.6×1.2 cm on the A3 scallop, with the latter associated with valve perforation. Additional small (<5 mm) vegetations were seen on the anterior and posterior MV leaflet chordae, along with moderate mitral regurgitation. It also confirmed an inferolateral left ventricle wall perforation and LVP formation with a neck measuring 0.8×0.9 cm. Adjacent to the neck, a 1.6×1.1 cm mobile, frayed, echogenic mass was seen in the left ventricular cavity attached to the endocardium of this wall, consistent with an intramural vegetation (*Figure 1E–I*). Serial imaging with CMR on day 5, CCTA on day 7 and TEE on day 8 did not demonstrate a clinically significant decrease in vegetation size; however, interpretation is limited because these measurements were obtained with different imaging modalities.

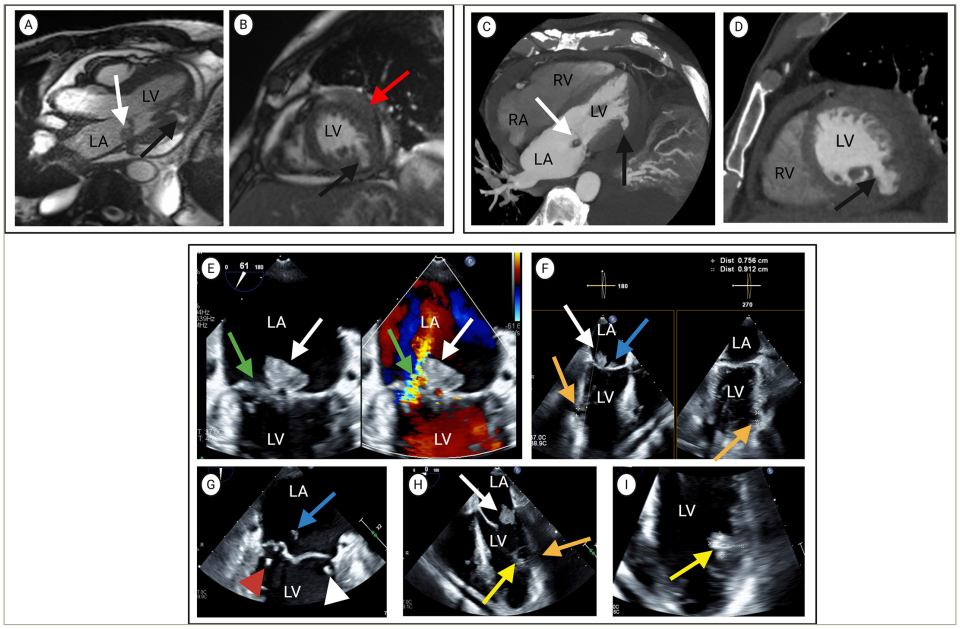
Management

A multidisciplinary heart team determined the timing of cardiovascular surgery. The patient underwent MV replacement with a 29 mm mosaic bioprosthetic valve and LVP repair using a bovine pericardial patch with pledgeted sutures on hospital day 16. Intraoperative findings confirmed anterior and lateral ventricular wall abscesses, LVP and extensive MV infection (*Figure 2A–C*). Histopathology confirmed IE with adjacent abscess and thrombus formation (*Figure 2D–G*). Subsequent analysis of the excised and debrided tissue showed *Streptococcus agalactiae*. Notably, fungal, anaerobic and acid-fast bacilli cultures were negative. The patient was then prescribed a 6-week course of ceftriaxone to be completed after his surgery.

Outcome and follow-up

The patient was discharged 7 days after his surgical repair to a rehabilitation facility for 2 weeks before returning home. Shortly afterward, he had a skin reaction to ceftriaxone for which he was switched to daptomycin and completed 6 weeks of antibiotics. He was subsequently enrolled in cardiac rehabilitation and has been doing well since. A summary of his clinical course is shown in *Figure 3*.

Figure 1: Multimodality imaging of infective endocarditis complicated by mitral valve vegetations, left ventricular abscess and left ventricular pseudoaneurysm



(A, B) Cardiovascular magnetic resonance steady-state free precession sequences
(A) Three-chamber long-axis and (B) mid-ventricular short-axis views demonstrate a left atrial vegetation attached to the posterior mitral leaflet (white arrow, 1.7×1.0 cm), inferolateral LV wall thinning with a pericardium-contained outpouching consistent with a left ventricular pseudoaneurysm (black arrow), and a 2.5×1.0 cm anterior LV wall abscess (red arrow).
(C, D) Cardiovascular computed tomography angiography
(C) Four-chamber long-axis and (D) short-axis views demonstrate the pseudoaneurysm in the mid-inferolateral left ventricle (black arrow) and a vegetation attached to the posterior mitral valve leaflet (white arrow).
(E–I) Transesophageal echocardiogram
(E) Mid-esophageal view shows vegetation on the posterior leaflet of the mitral valve measuring 2.0×1.2 cm (white arrow) with leaflet perforation (green arrow) and regurgitant jet from the left ventricle to the left atrium. (F) Mid-esophageal biplane views show vegetation on the mitral valve anterior leaflet (blue arrow), posterior leaflet (white arrow) and left ventricular pseudoaneurysm (orange arrow). (G) Mid-esophageal view shows vegetations on the mitral valve anterior leaflet measuring 0.6×1.2 cm (blue arrow), anterior leaflet chordae (white arrowhead) and posterior leaflet chordae (red arrowhead). (H) Mid-esophageal view shows vegetation on the mitral valve posterior leaflet (white arrow) and mural left ventricular wall vegetation (yellow arrow) with an adjacent pseudoaneurysm (orange arrow). (I) Mid-esophageal view shows mural vegetation on the left ventricular inferolateral wall measuring 1.1×1.6 cm (yellow arrow)
LA = left atrium; LV = left ventricle; RA = right atrium; RV = right ventricle.

Discussion

Formation of LVP from IE is exceedingly rare and is associated with high morbidity and mortality. The most common cause of LVP is transmural myocardial infarction, followed by iatrogenic cardiac injury after surgery and complications of IE. LVP occurs when a myocardial rupture is contained by the pericardium, fibrin, hematoma or scar tissue. Unlike LVP (wall perforation with a narrow-neck defect covered by pericardium and thrombus forming a saccular cavity), a true ventricular aneurysm has no wall rupture but outpouching and dyskinesis of the scarred wall with thinned, fibrotic but continuous myocardium containing all three layers (endocardium, myocardium and epicardium).[3]

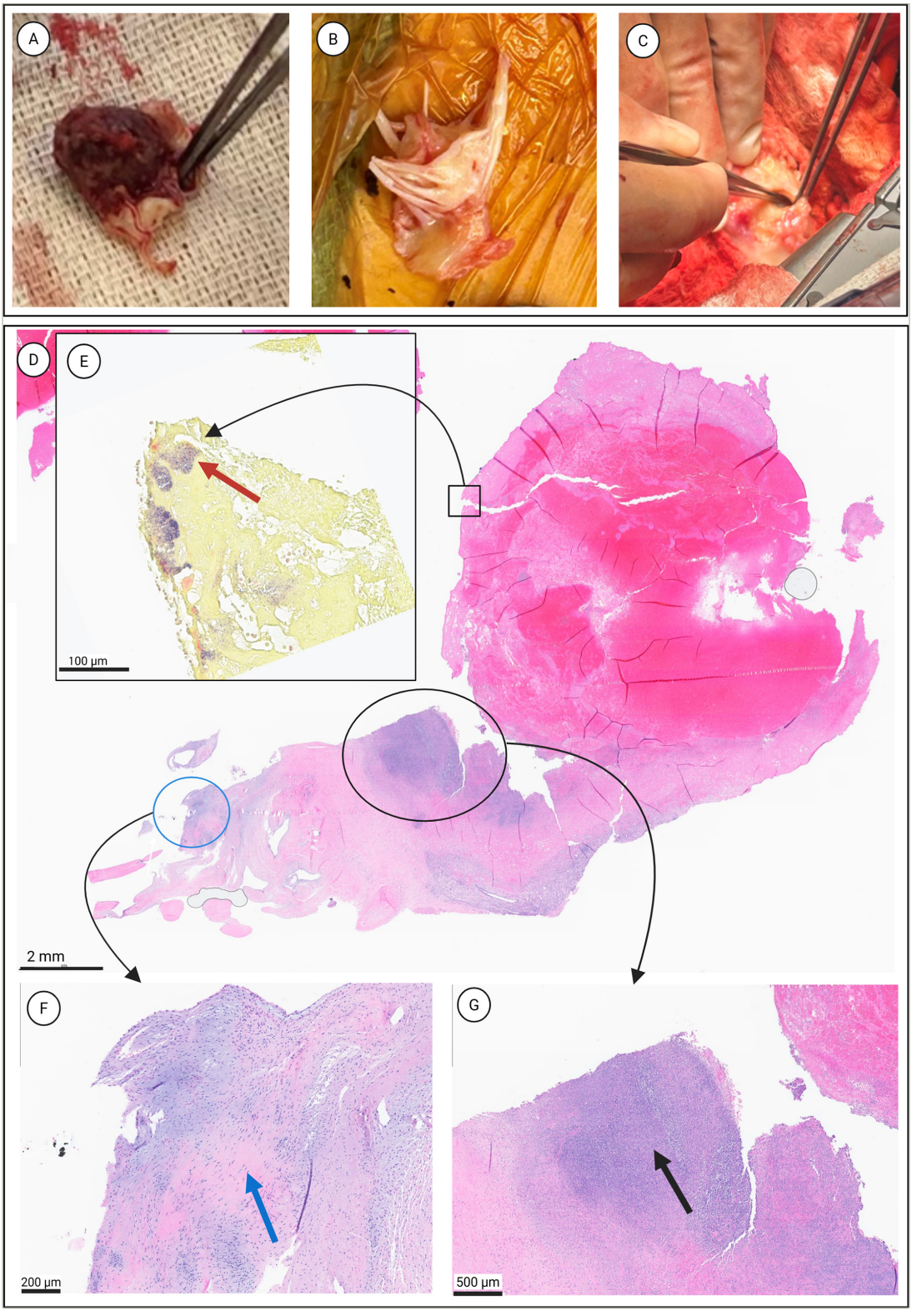
Native valve endocarditis secondary to *Streptococcus agalactiae* is uncommon in healthy, immunocompetent individuals without preexisting valvular disease. In this case, bacteremia likely originated from a genitourinary source, progressing to endocarditis facilitated by host immune dysfunction from poorly controlled diabetes and chronic HIV.[4] Patients with LVP can be asymptomatic or symptomatic with dyspnea, chest pain or overt heart failure. This heterogeneity makes diagnosis challenging, highlighting the importance of high clinical suspicion.[3]

The pathophysiology of IE-associated LVP involves two primary mechanisms: direct hematogenous microbial myocardial seeding or periannular abscess extension, most commonly from the mitral or aortic valve.[5,6] Once established, the infection can expand into the myocardial tissue, catalyzed by high left ventricular systolic pressure, myocardial erosion by bacterial toxins, matrix-degrading proteases and immune-mediated injury. These factors mechanically disrupt and weaken the ventricular wall. Ultimately, progressive myocardial breakdown culminates in either ventricular free-wall rupture with tamponade and sudden death or a contained rupture (pseudoaneurysm).[3] As this process develops gradually, clinicians should remain vigilant for myocardial involvement in patients with IE even with negative initial imaging, especially if clinical deterioration occurs.[3]

Accurate IE diagnosis and detection of complications require a multimodal approach, particularly with atypical organisms, subtle initial findings or extracardiac complications. TTE is the initial imaging modality for diagnosing IE, but it has operator variability and a relatively low sensitivity of approximately 60%.[7] In most cases, additional imaging is necessary. Our patient's initial TTE missed all significant IE findings, which were later appreciated with a multimodal imaging approach, despite poor image quality. TEE has greater sensitivity (>90%) but is semi-invasive and may miss very small vegetations (<2 mm) or certain IE sequelae (e.g. perivalvular abscess) in 10–20% of patients.[8] Consequently, imaging studies such as CCTA and CMR are potential adjuncts in complex or ambiguous cases.

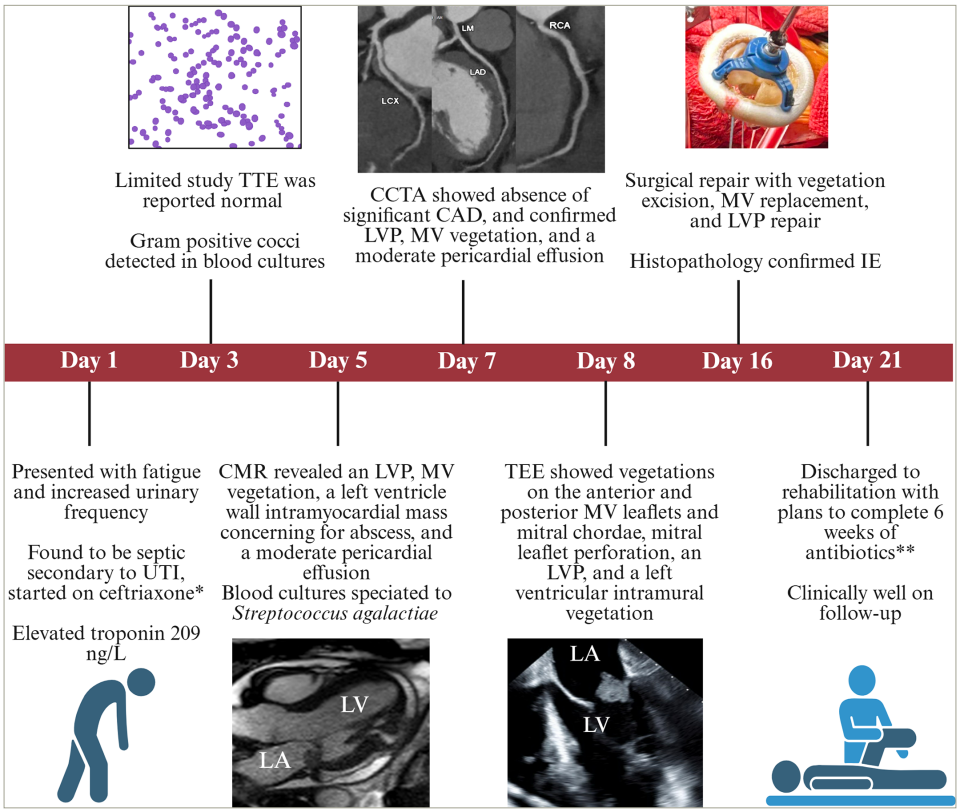
CCTA and CMR provide unique advantages, complementing echocardiography. CCTA provides excellent spatial resolution of cardiac structures, pericardium and coronary arteries.[9] In patients with obesity or chronic obstructive pulmonary disease, where TTE image quality is often limited, CCTA and CMR maintain high diagnostic performance while being noninvasive.[10] CMR provides excellent visualization of cardiac anatomy,

Figure 2: Surgical and histopathologic correlation of infective endocarditis with mitral valve destruction and left ventricular pseudoaneurysm



(A–C) Intraoperative findings
(A) Excised 2×2 cm mitral valve vegetation
(B) Excised remnant of the posterior leaflet of the mitral valve with adjacent chordae
(C) Inferolateral left ventricular wall at surgery, showing the pseudoaneurysm
(D–G) Histopathology
(D) Low-power view (1×) of the posterior basal mitral valve leaflet from the atrial side, demonstrating myxoid degeneration of the valvular tissue (blue circle) and an adjacent abscess cavity with necro-inflammatory debris (black circle), consistent with infective endocarditis. The boxed area indicates the region from which the Gram stain was obtained
(E) Inset: high-power (40×) Gram stain showing clusters of Gram-positive cocci (red arrow)
(F) Higher power view (10×) corresponding to the myxoid region marked by the blue circle in panel D, demonstrating expanded, pale myxoid stroma with dispersed spindle cells, characteristic of myxoid degeneration (blue arrow)
(G) Higher power view (5×) corresponding to the abscess region marked by the black circle in panel D, showing a well-formed valvular abscess with dense neutrophilic infiltration and necrosis (black arrow)

Figure 3: Timeline of clinical course



** Ceftriaxone 2 g IV push q24*
*** Started on Ceftriaxone 2 g IV q24 but switched to daptomycin 750 mg IV q24 due to skin reaction*
CAD = coronary artery disease; CCTA = cardiovascular computed tomography angiography; CMR = cardiovascular magnetic resonance imaging; hsTnI = high-sensitivity troponin I; IE = infective endocarditis; LVP = left ventricular pseudoaneurysm; MV = mitral valve; TTE = transthoracic echocardiogram; TEE = transesophageal echocardiogram; UTI = urinary tract infection.

structure and function, plus unmatched tissue characterization, late gadolinium enhancement and T1/T2 mapping detect edema, inflammation, viability and scarring.[11] Furthermore, CMR avoids ionizing radiation, which is particularly important for younger or pregnant patients or those needing serial imaging. Together, these modalities provide complementary anatomic and functional insights, enhancing diagnostic precision.

Conclusion

Our case illustrates the importance of multimodal imaging in a unique presentation. Initial TTE was nondiagnostic despite ECG and laboratory evidence of myocardial injury. CMR obtained to evaluate for myopericarditis and myocardial infarction with non-obstructive coronary arteries (MINOCA) incidentally revealed the LVP. CCTA confirmed coronary patency and excluded an ischemic etiology, while TEE revealed multiple valvular vegetations and an intramural echogenic mass/abscess. These complementary modalities enabled accurate recognition of pathological extent and informed surgical planning. This multimodal approach transformed an ambiguous initial presentation into a clear diagnosis with an actionable treatment plan, ultimately leading to a successful repair.

Patient's perspective

The patient described the illness as a frightening experience, particularly because the initial symptoms seemed mild and nonspecific. He reported feeling reassured once the diagnosis was clarified, and the treatment plan was explained by the care team. Following surgery and rehabilitation, he noted progressive recovery in his energy levels and daily activities. He expressed appreciation for the multidisciplinary care he received and the support provided during his recovery. ❑

1. Delgado V, Ajmone Marsan N, De Waha S, et al. 2023 ESC guidelines for the management of endocarditis. *Eur Heart J*. 2023;44:3948–4042. DOI: 10.1093/eurheartj/ehad193.
2. Yeh T-C, Liu C-P, Tseng C-J, et al. Left ventricular pseudoaneurysm caused by infective endocarditis. *Acta Cardiol Sin*. 2014;30:346–9.
3. Frances C, Romero A, Grady D. Left ventricular pseudoaneurysm. *J Am Coll Cardiol*. 1998;32:557–61. DOI: 10.1016/s0735-1097(98)00290-3.
4. Alexander M, Cho E, Gliozheni E, et al. Pathology of diabetes-induced immune dysfunction. *Int J Mol Sci*. 2024;25:7105. DOI: 10.3390/ijms25137105.
5. Hu W, Wang X, Su G. Infective endocarditis complicated by embolic events: Pathogenesis and predictors. *Clin Cardiol*. 2021;44:307–15. DOI: 10.1002/clc.23554.
6. Baumann AA, Lushington J, Pitman BM, et al. A case of left ventricular outflow tract pseudoaneurysm: An incidental finding revealing occult infective endocarditis. *CASE (Phila)*. 2020;4:401–4. DOI: 10.1016/j.case.2020.05.008.
7. Bai AD, Steinberg M, Showler A, et al. Diagnostic accuracy of transthoracic echocardiography for infective endocarditis findings using transesophageal echocardiography as the reference standard: a meta-analysis. *J Am Soc Echocardiogr*. 2017;30:639–46. DOI: 10.1016/j.echo.2017.03.007.
8. Gomes A, Glaudemans AWJM, Touw DJ, et al. Diagnostic value of imaging in infective endocarditis: A systematic review. *Lancet Infect Dis*. 2017;17:e1–14. DOI: 10.1016/S1473-3099(16)30141-4.
9. Khalique OK, Veillet-Chowdhury M, Choi AD, et al. Cardiac computed tomography in the contemporary evaluation of infective endocarditis. *J Cardiovasc Comput Tomogr*. 2021;15:304–12. DOI: 10.1016/j.jcct.2021.02.001.
10. Mangold S, Wichmann JL, Schoepf UJ, et al. Diagnostic accuracy of coronary CT angiography using 3rd-generation dual-source CT and automated tube voltage selection: Clinical application in a non-obese and obese patient population. *Eur Radiol*. 2017;27:2298–308. DOI: 10.1007/s00330-016-4601-2.
11. Dursun M, Yılmaz S, Yılmaz E, et al. The utility of cardiac MRI in diagnosis of infective endocarditis: Preliminary results. *Diagn Interv Radiol*. 2015;21:28–33. DOI: 10.5152/dir.2014.14239.